RESEARCH ARTICLE

▪ Vol. 5, No. 1 (Winter 2024)
▪ Pages: 1 – 8
▪ p-ISSN: 2791-0245
▪ e-ISSN: 2791-0229
▪ DOI: 10.55737/qjssh.406280930

Open Access

QLANTIC JOURNAL OF SOCIAL SCIENCES AND HUMANITIES

Examining the Insight Impacts of Indian Ocean Pressure on Autumntime Precipitation Variability over Tasmania through Singular Value Decomposition Analysis

Kamran Khan[1] Saqib-Ur-Rehman[2] Muhammad Zulqarnain Siddiqui[3] Atia Elahi[4] Abdul Jameel Khan[5]

Abstract: *This study explores further the impacts of the relationship between autumntime mean sea level pressure (MSLP) over the Indian Ocean and autumntime precipitation over Tasmania. We employ a combination of cross-correlation analysis, Singular Value Decomposition (SVD), and covariance measures to unravel this intricate connection. Our results reveal that MSLP over the Indian Ocean significantly influences Tasmania's autumn precipitation, particularly in the region extending from 125°E eastward and from 35°S southward. This MSLP-precipitation link is statistically significant, characterized by a Pearson's coefficient of correlation of 0.63 ($p < 0.05$). In addition, we calculate the Root Mean Square Covariance (RMSC) to gauge the strength of this association. The RMSC value, calculated at 0.33, surpasses the threshold of 0.1, emphasizing a robust and significant connection between autumntime MSLP and precipitation in Tasmania. Our results emphasize that the first leading mode of SVD accounts for 84% of the variability in both MSLP over the Indian Ocean and precipitation in Tasmania. These results contribute to a more profound understanding of the factors governing autumn precipitation in Tasmania and offer valuable insights for meteorological and climate science.*

Key Words: Singular Value Decomposition, Square Covariance Fraction, Mean Sea Level Pressure, Topographical Influence, Climate Variability

Introduction

Tasmania is situated in the southeastern region of Australia. Geographically, it encompasses mountainous terrain in its western parts, while the eastern regions consist of relatively low plains. This distinctive orographic feature greatly influences the east-west precipitation patterns (Rehman et al., 2019). For instance, the western regions experience higher levels of precipitation compared to the eastern regions of the state (Hill et al., 2009; Tozer et al., 2018; Lewis et al., 2018). The high mountains in western Tasmania play a pivotal role in hydro-electricity production, making them a significant contributor to Australia's hydro-electricity generation (Lewis et al., 2018).

The spatial distribution of autumntime (March to May; MAM) seasonal total precipitation across the island is visually represented in Figure 1. This graphical depiction clearly shows that autumntime precipitation in the western parts typically falls within the range of 200mm to 900 mm, whereas in the central and eastern areas, it typically ranges from 100mm to 300 mm. Notably, the precipitation values in the entire island exceed the seasonal average and highly variable precipitation (Figure 2). One of the key findings of Rehman et al. (2019) indicates a temporal trend, with autumn precipitation showing the lowest levels when compared to the other seasons (summer, winter, and spring) in Tasmania from 1951 to 2016. This trend is statistically significant at a p-value of less than 0.05. In a similar vein, Cai et al. (2013) also noted a substantial decline in autumn precipitation over southeastern Australia, which includes Tasmania, dating back to the 1950s.

[1] Assistant Professor, Department of Computer Science, Iqra University, Karachi, Sindh, Pakistan.
[2] Assistant Professor, Department of Mathematics, University of Karachi, Karachi, Sindh, Pakistan.
[3] Assistant Professor, Department of Computer Science, Iqra University, Karachi, Sindh, Pakistan.
[4] Lecturer, Department of Business Administration, Iqra University, Karachi, Sindh, Pakistan.
[5] Assistant Professor, Department of Computer Science, Iqra University, Karachi, Sindh, Pakistan.

▪ **Corresponding Author:** Kamran Khan (kamrankhan@iqra.edu.pk)
▪ **To Cite:** Khan, K., Rehman, S. U., Siddiqui, M. Z., Elahi, A., & Khan, A. J. (2024). Examining the Insight Impacts of Indian Ocean Pressure on Autumntime Precipitation Variability over Tasmania through Singular Value Decomposition Analysis. *Qlantic Journal of Social Sciences and Humanities, 5*(1), 1-8. https://doi.org/10.55737/qjssh.406280930

Figure 1

Depicts the total precipitation over Tasmania, Australia, specifically during the autumn season, covering the time span from 1951 to 2020.

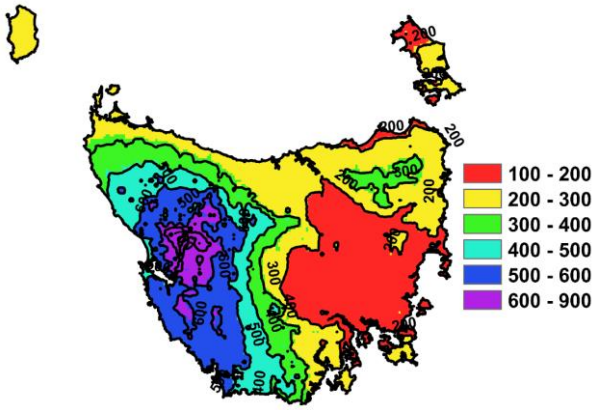

The impact of global atmospheric circulations on autumntime climate variability in Southeastern Australia (SEA) is elucidated in the work of Cai et al. (2013), with a specific focus on Tasmania (Rehman et al., 2019; Tozer et al., 2018; Chubb et al., 2018; Hill et al., 2009). These studies collectively conclude that the Southern Annular Mode (SAM) is not directly associated with the decline in autumn precipitation. However, there is an association between the SAM and decreased winter precipitation over South Australia, Victoria, and certain parts of Tasmania, as highlighted by Meneghini et al. (2007). The SAM's impact is particularly noteworthy in western Tasmania, while the Pacific South American (PSA) mode, as outlined by Irving et al. (2016), and the El-Nino Southern Oscillation (ENSO) exhibit a state-wide impact, as noted by Hill et al. (2009). A decrease in precipitation across all seasons is attributed to the progressive segment of SAM in western Tasmania. Moreover, increased seasonal precipitation, except during summer, in southwestern Tasmania is correlated with the influx of westerly and southwesterly air streams, as explained by Chubb et al. (2018), while blocking systems hinder these air streams, as found by Risbey et al. (2009).

Figure 2

Illustrates the standard deviation of precipitation during the autumn season

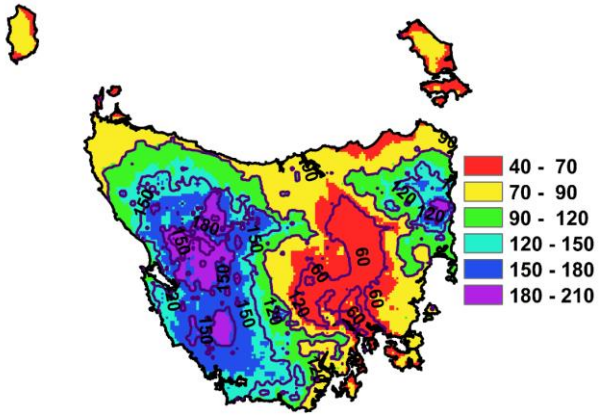

The variability in SEA's autumn precipitation is partly attributable to ENSO, SAM, and the destructive segment of the Indian Ocean Dipole (IOD), as reported by Timbal et al. (2013). During the progressive (destructive) segments of IOD, Australia experiences low (high) precipitation anomalies in various regions. Conversely, the negative phase of IOD results in greater precipitation anomalies in SEA, including Tasmania and Western Australia.

Tozer et al. (2018) conducted a comparative analysis of extreme rainfall events at two rainfall stations, Queenstown and Fingal, located in Tasmania. These stations were strategically selected to investigate the association between the east-west gradient of extreme precipitation over the island, with Queenstown representing the west and Fingal representing the east. The study's key finding revealed that the relatively low variance accounting for the east-west gradient in extreme precipitation across the island is primarily attributed to the influence of Rossby waves. The investigation focused on daily wintertime precipitation

(April to October) in western Tasmania for the years 2014 and 2015. Among the findings, the study identified a significant correlation between daily wintertime precipitation and wind speed at an altitude of 1000 meters over a reference point located 100 kilometres off the west coast of the state, as detailed by Lewis et al. (2018).

Figure 3 (a)

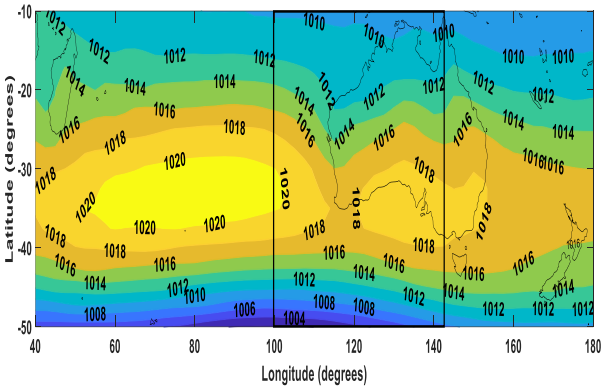

Figure 3 (b)

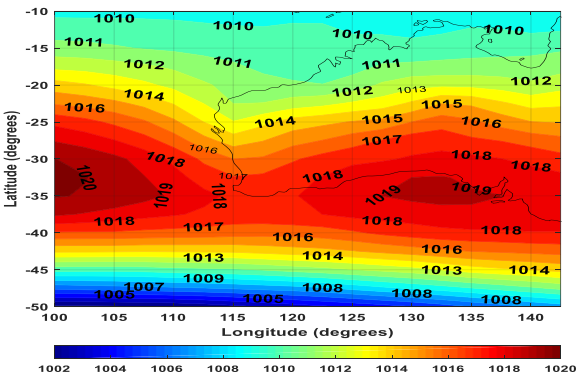

Figure 3 Illustration of the MSLP field in the Indian Ocean region during the autumn season. In part (a), the entire domain is shown, with the area of our study enclosed within a black outlined square. In part (b), a closer view of the study square area, which is associated with precipitation in Tasmania, is presented.

Timbal et al., (2013) suggested that the intensity and pole-ward shift of subtropical ridge (STR) is significantly related to change in seasonal precipitation over SEA. The evidence found by Rehman et al., (2019) that strength of IOH_P and its zonal movement strongly influenced the autumntime seasonal precipitation over Tasmania. The findings from the study conducted by Tozer et al. (2018) suggest an association between coherent large-scale atmospheric wave patterns and both dry and wet precipitation maxima in Tasmania. Lewis et al. (2018) studied the formation of precipitation, both theoretically and by utilizing computer models, due to the continual rainfall in western Tasmania, which is unique across Australia. Three distinct weather patterns are responsible for the varying amounts of rainfall in Tasmania, which is located in the southern hemisphere. These patterns are called ENSO, SAM, and PSA. Some of the major studies presented on the Tasmanian climate indicated these findings (Rehman et al., 2019; Tozer et al., 2018; Lewis et al., 2018; Hill et al., 2009).

Data and Methodology

We acquired monthly precipitation gridded high resolution (0.05°) data for the period of 1951 to 2020 for the autumn season for the domain of Tasmania, Australia. This data was constructed by the Australian Bureau of Meteorology (Jones et al. 2009) and obtained from the Australian Water Availability Project (AWAP). Additionally, in this study, MSLP data covering the Indian Ocean domain were sourced from the National Centers for Environmental Prediction (NCEP). The averaged MSLP field for autumn over the Indian Ocean is illustrated in Figure 3a from 1951 to 2020.

The present study aims to identify linear combinations that can explain the maximum possible covariance between the MSLP field and autumntime precipitation over Tasmania. Based on the obtained coefficients, the study explores the spatial distribution of covariance within these fields. To achieve this objective, SVD is employed with these datasets. This technique proves to be straightforward and applicable when the goal is to uncover the maximum covariance between two data sets, as previously discussed by Cherry (1997). This approach is particularly valuable when dealing with geophysical observations (Riaz et al., 2017). It's worth noting that SVD has found applications in numerous studies, including those by Kisesa et al. (2020), Qi et al. (2018), Riaz et al. (2017), Syed et al. (2006), Klopper et al. (1998), Bretherton et al. (1992), Björnsson et al. (1997), and Wallace et al. (1992).

Before applying SVD, we construct the covariance matrix C_{XY}, representing the relationship between MSLP and autumntime precipitation over Tasmania (AP). Here, the left and right time series are

symbolized as X and Y, respectively. In this context, the left time series (Figure 3b) corresponds to MSLP, while the right time series represents autumntime precipitation over Tasmania (AP). The MSLP observations are gathered within a specific rectangular domain located over the Indian Ocean (Figure 3b). This domain spans longitudes from 100°E to 142.5°E and latitudes from 10°S to 50°S and is derived from the work of Rehman et al. (2019).

The mathematical expression for the covariance matrix C_{XY} is defined as follows:

$AP = U^t \mathbf{X}$

$Mslp = V^t \mathbf{Y}$

$c = cov\,[AP, Mslp] = cov[U^t \mathbf{X}, V^t \mathbf{Y}] = \frac{1}{n-1}\,[U^t \mathbf{X}\,(V^t \mathbf{Y})^t] = U^t C_{xy} V$

$C_{xy} = \frac{1}{n-1}\,\mathbf{X}\mathbf{Y}^t$

The covariance matrix C_{XY} is subjected to decomposition using the SVD method, resulting in three orthogonal matrices. Among these, the two vectors, U(t) and V(t), constitute the singular vectors. The third matrix is the diagonal matrix denoted as "S," which comprises the singular values, also known as eigenvalues. Within U(t) and V(t), the jth columns contain left (u_j) and right (v_j) singular vectors, while a jth element of the diagonal matrix S represents the singular value of Xu_j and Yv_j. These vectors, Xu_j and Yv_j, signify the jth pair of SVD expansion coefficients for the left and right fields, respectively, where n indicates the number of observations.

To illustrate, when j equals 1, the first pair of expansion coefficients, also referred to as the first mode, elucidates the maximum achievable square covariance fraction (SCF) between the fields, with subsequent pairs explaining progressively less covariance than their predecessors, as detailed in many studies (Zhang et al., 2018; Syed et al., 2006; Bretherton et al., 1992). Additionally, it's important to note that each subsequent mode also describes a distinct spatial pattern in comparison to the preceding mode. The first leading duo of patterns is selected to maximize the covariance, achieved by projecting the extended value of the left field for the first leading mode onto the extended value of the right field, following the approach outlined in the work of Riaz et al. (2017), Bretherton et al. (1992) and Klopper et al. (1998).

Result and Discussions

The autumntime seasonal precipitation index for the Tasmanian region and the MSLP in the Indian Ocean region (spanning from 100° to 142.5° E and 10° to 45° S) are derived through the accumulation of monthly total precipitation and the averaging of monthly sea level pressure, respectively. This process is carried out over the months of March to May (MAM) in the years from 1951 to 2020. Subsequently, a cross-correlation matrix is calculated by the autumntime MSLP over the Indian Ocean and precipitation over Tasmania.

Table 1

Representation of the SCF, cumulative square covariance fraction (CSCF), and correlation coefficients between the extended values of the first three leading modes of SVD

Mode	SCF%	CSCF%	Pearson's Correlation
1	84.00	84.00	0.72
2	15.00	99.00	0.56
3	0.44	99.44	0.30

** Note: Values are significant at the p < 0.05 level.*

SVD is applied by using the cross-correlation matrix, resulting in the identification of the three leading SVD modes that account for 99.44% of the total squared covariance, as presented in Table 1. Rehman's (2014) work is dedicated to the analysis of the initial principal component analysis mode, which explained a significant 84.43% of the overall inconsistency in streamflow within the southwestern region of Australia. In this context, the SCF of the first leading mode was selected due to its ability to explain 84% of the coupled covariance.

The correlation coefficients between the extended values of the MSLP and precipitation fields are detailed in Table 1. These coefficients indicate the strength of the associations between the modes.

Specifically, the correlation coefficients between the first, second, and third extended values are 0.72, 0.56, and 0.30, respectively. These associations exhibit statistical significance with a p-value of less than 0.05. The coefficient of determination (R-square variance) of these associations is evaluated as 51.84%, 31.36%, and 9%, respectively. These correlation coefficients shed light on the intensity of the linear relationships between the extended values of the coupled modes. Based on these coefficients, it can be estimated that the extended values of the first leading mode in the MSLP field (left) explain 51.84% of the total variance in the first mode of the extended coefficients of the precipitation field (right). Moreover, the highest correlation value for the first leading mode suggests its greater importance among the SVD modes. Furthermore, the second leading mode contributes to 31.36% of the total variance, and the third leading mode elucidates 9% of the total variance in the extended values of the coupled modes.

Figure 4 (a)

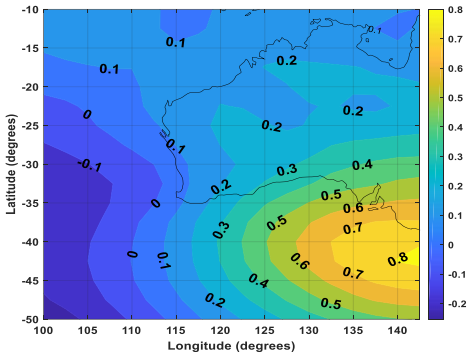

Figure 4 (b)

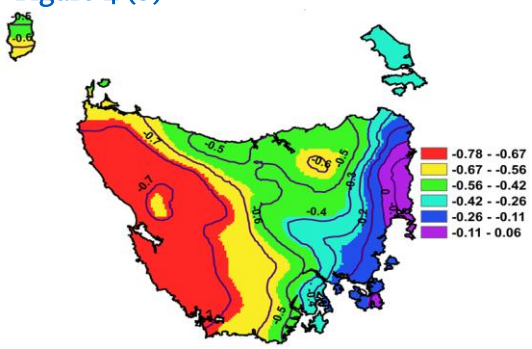

Figure 4 Illustration of the correlation (heterogeneous) coefficients' contour maps (a) the correlation between MSLP of the Indian Ocean pressure field and the extended values of the right field (precipitation) for the first leading mode of SVD, and (b) the correlation between precipitation and the extended values of the left field (MSLP of the Indian Ocean pressure field) for the same first leading mode.

The heterogeneous correlations of the first mode are visually depicted in Figure 4. These figures elucidate the spatial patterns that represent the strength of the associations between the left and right fields. In Figure 4a, it is evident that autumn-time precipitation (the right field) exhibits a stronger association with sea level pressure (left field) from the region spanning 125°E and further eastward and from 35°S and extending further southward.

Figure 4b, on the other hand, provides insights into how effectively the Indian Ocean pressure system explains autumn precipitation variability over Tasmania. It can be interpreted as suggesting that the entirety of autumntime precipitation over the island is linked to Indian Ocean MSLP, except for a northeastern strip of the island where the correlation coefficients are notably weaker. Tasmania receives most of the rainfall in the northeastern areas from the cutoff lows developed in the Tasman Sea (Pook et al., 2010; Risbey et al., 2009; Risbey et al., 2013; Bennet et al., 2010).

Figure 5

Illustration of the comparative analysis between the normalized average March to May (MAM) time series of precipitation over Tasmania

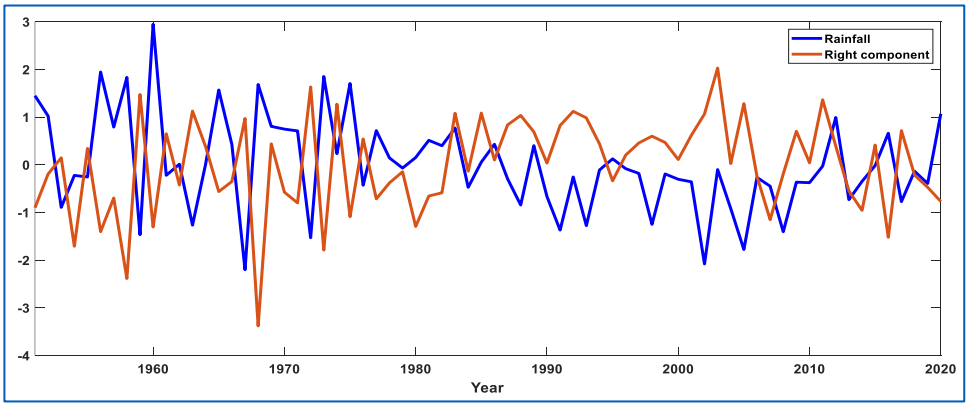

Illustration of the comparative analysis between the normalized average March to May (MAM) time series of precipitation over Tasmania and the normalized time series of the coefficients of expansion for the right field (precipitation) in the first leading mode of SVD. The association between the series is 0.63, signifying statistical significance at the $p < 0.05$ threshold.

The temporal patterns of autumntime precipitation (right field) and its associated extended values are visually presented in Figure 5. The observed similarities in the fluctuations of both time series highlight the robust relationship between them. This strong relationship is quantified by a homogeneous correlation coefficient of 0.63, signifying the closeness of the association between the series. Importantly, this correlation is significant at a 5% statistical level. Furthermore, the temporal patterns of the first mode of autumntime sea level pressure (the SVD left field scores) and the first mode of precipitation over Tasmania (the SVD right field scores) are also depicted in Figure 6.

Figure 6

Time series analysis for the extended values of the first leading mode in the SVD.

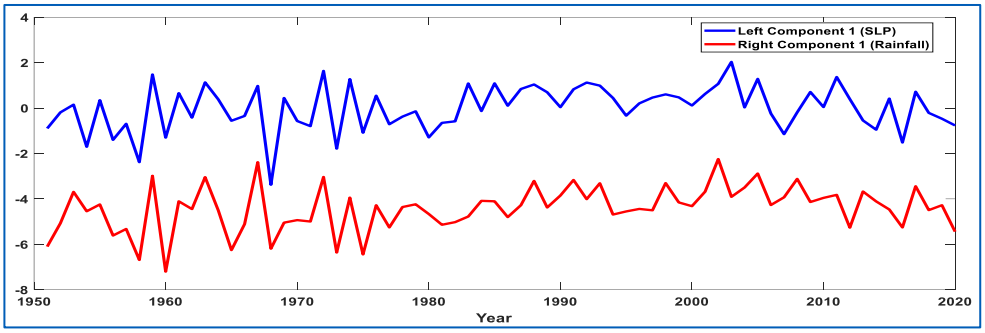

Time series analysis for the extended values of the first leading mode in the SVD. The association between time series is found to be 0.72, which is significant at a 5% statistical level.

In this study, it is imperative to calculate the RMSC as part of the correlation analysis. RMSC serves as a critical metric for assessing the strength of the magnitude of association between the fields under study. A value of 0.1 or higher for RMSC indicates a strong correlation between the two fields, as outlined by Wallace et al. in 1992. In the context of this study, the RMSC value is determined to be 0.33, surpassing the established threshold of 0.1. This result strongly suggests a robust and significant relationship between autumn-time sea level pressure and autumn-time precipitation over Tasmania.

Summary and Conclusion

In 2019, Rehman et al. established a connection between the autumn Indian Ocean high-pressure system, characterized by the mean central pressure, and autumn precipitation in Tasmania. They utilized the Center of Action (COA) approach for this investigation. Their study also revealed that the relationship between the autumn high-pressure system in the Indian Ocean and autumn precipitation on the island is notably stronger and significant at the $p < 0.05$ statistical level when compared to other seasons (summer, winter, and spring). This study further explores the specific modes of association, focusing on which domain within the Indian Ocean, as depicted in Figure 3b, is more prominently linked to this relationship in terms of variability. This exploration is conducted using SVD analysis.

The study delves into the relationship between autumntime MSLP over the Indian Ocean and autumntime precipitation in Tasmania. A cross-correlation matrix was constructed for both datasets, and SVD was applied to analyze them. This process resulted in both left and right singular vectors alongside a diagonal matrix that holds singular values.

These singular vectors were then used to calculate the left and right SVD scores, with the right SVD score reflecting the projection of autumntime precipitation on the right singular vector and the left SVD score computed using autumntime MSLP and the left singular vector. The study also involved calculating correlation coefficients for the first three SVD scores, SCF and CSCF, to quantify the strength of associations between variables.

Furthermore, RMSC was used to assess the impact of the relationship between the coupled fields. A heterogeneous correlation contour plot in Figure 4 visually illustrates the degree to which one field can explain the other. Notably, the first dominant mode displayed an SCF of 84%, indicating that it alone explained 84% of the variance in autumntime MSLP over the Indian Ocean and autumntime precipitation in Tasmania.

References

Bennett, J. C., Ling, F. L. N., Graham, B., Grose, M. R., Corney, S. P., White, C. J., ... & Bindoff, N. L. (2010). Climate Futures for Tasmania: water and catchments technical report. *Antarctic Climate & Ecosystems Cooperative Research Centre, Hobart, Tasmania*.

Björnsson, H., & Venegas, S. A. (1997). A manual for EOF and SVD analyses of climatic data. *CCGCR Report*, *97*(1), 112-134. https://paleodyn.uni-bremen.de/gl/geo_html/lehre/eof/hart/eofsvd.html

Bretherton, C. S., Smith, C., & Wallace, J. M. (1992). An intercomparison of methods for finding coupled patterns in climate data. *Journal of climate*, *5*(6), 541-560. https://doi.org/10.1175/1520-0442(1992)005<0541:AIOMFF>2.0.CO;2

Cai, W., & Cowan, T. (2013). Southeast Australia Autumn rainfall reduction: A climate-change-Induced Poleward shift of ocean–atmosphere circulation. *Journal of Climate*, *26*(1), 189-205. https://doi.org/10.1175/jcli-d-12-00035.1

Cherry, S. (1997). Some comments on singular value decomposition analysis. *Journal of Climate*, *10*(7), 1759-1761. https://doi.org/10.1175/1520-0442(1997)010<1759:scosvd>2.0.co;2

Chubb, T. H., Siems, S. T., & Manton, M. J. (2011). On the decline of wintertime precipitation in the snowy mountains of southeastern Australia. *Journal of Hydrometeorology*, *12*(6), 1483-1497. https://doi.org/10.1175/jhm-d-10-05021.1

Hill, K. J., Santoso, A., & England, M. H. (2009). Interannual tasmanian rainfall variability associated with large-scale climate modes. *Journal of Climate*, *22*(16), 4383-4397. https://doi.org/10.1175/2009jcli2769.1

Irving, D., & Simmonds, I. (2016). A new method for identifying the Pacific–south American pattern and its influence on regional climate variability. *Journal of Climate*, *29*(17), 6109-6125. https://doi.org/10.1175/jcli-d-15-0843.1

Jones, D., Wang, W., & Fawcett, R. (2009). High-quality spatial climate data-sets for Australia. *Australian Meteorological and Oceanographic Journal*, *58*(04), 233-248. https://doi.org/10.22499/2.5804.003

Kisesa, M., Umutoni, M., Japheth, L., Lipiki, E., Kebacho, L., & Tilwebwa, S. (2020). The covariability of sea surface temperature and MAM rainfall on East Africa using singular value decomposition analysis. *Geographica Pannonica*, *24*(4), 261-270. https://doi.org/10.5937/gp24-27577

Klopper, E., Landman, W. A., & Van Heerden, J. (1998). The predictability of seasonal maximum temperature in South Africa. *International Journal of Climatology*, *18*(7), 741-758. https://doi.org/10.1002/(sici)1097-0088(19980615)18:7<741::aid-joc279>3.0.co;2-b

Lewis, C., Huang, Y., Siems, S., & Manton, M. (2018). Wintertime orographic precipitation over western Tasmania. *Journal of Southern Hemisphere Earth System Science*, *68*(1), 22-40. https://doi.org/10.22499/3.6801.003

Meneghini, B., Simmonds, I., & Smith, I. N. (2006). Association between Australian rainfall and the southern annular mode. *International Journal of Climatology*, *27*(1), 109-121. https://doi.org/10.1002/joc.1370

Pook, M., Risbey, J., & McIntosh, P. (2010). East Coast lows, atmospheric blocking and rainfall: A tasmanian perspective. *IOP Conference Series: Earth and Environmental Science*, *11*, 012011. https://doi.org/10.1088/1755-1315/11/1/012011

Qi, P., Zhang, G., Xu, Y., Wang, L., Ding, C., & Cheng, C. (2018). Assessing the influence of precipitation on shallow groundwater table response using a combination of singular value decomposition and cross-wavelet approaches. *Water*, *10*(5), 598. https://doi.org/10.3390/w10050598

Rehman, S. U. (2014). Influence of Indian Ocean high pressure on streamflow variability over southwestern Australia. *Annals of Geophysics*, *57*(2), P0212-P0212. https://doi.org/10.4401/ag-6398

Rehman, S. U., Khan, K., & Simmonds, I. (2019). Links between tasmanian precipitation variability and the Indian Ocean subtropical high. *Theoretical and Applied Climatology*, *138*(3-4), 1255-1267. https://doi.org/10.1007/s00704-019-02891-z

Riaz, S. M., & Iqbal, M. J. (2016). Singular value decomposition analysis for examining the impact of siberian high on winter precipitation variability over South Asia. *Theoretical and Applied Climatology*, *130*(3-4), 1189-1194. https://doi.org/10.1007/s00704-016-1948-x

Risbey, J. S., McIntosh, P. C., & Pook, M. J. (2012). Synoptic components of rainfall variability and trends in southeast Australia. *International Journal of Climatology*, *33*(11), 2459-2472. https://doi.org/10.1002/joc.3597

Risbey, J. S., Pook, M. J., McIntosh, P. C., Wheeler, M. C., & Hendon, H. H. (2009). On the remote drivers of rainfall variability in Australia. *Monthly Weather Review*, *137*(10), 3233-3253. https://doi.org/10.1175/2009mwr2861.1

Syed, F. S., Giorgi, F., Pal, J. S., & King, M. P. (2006). Effect of remote forcings on the winter precipitation of central Southwest Asia Part 1: Observations. *Theoretical and Applied Climatology*, *86*(1-4), 147-160. https://doi.org/10.1007/s00704-005-0217-1

Timbal, B., & Drosdowsky, W. (2012). The relationship between the decline of southeastern Australian rainfall and the strengthening of the subtropical ridge. *International Journal of Climatology*, *33*(4), 1021-1034. https://doi.org/10.1002/joc.3492

Tozer, C. R., Risbey, J. S., O'Kane, T. J., Monselesan, D. P., & Pook, M. J. (2018). The relationship between wave trains in the southern hemisphere storm track and rainfall extremes over Tasmania. *Monthly Weather Review*, *146*(12), 4201-4230. https://doi.org/10.1175/mwr-d-18-0135.1

Ummenhofer, C. C., England, M. H., McIntosh, P. C., Meyers, G. A., Pook, M. J., Risbey, J. S., Gupta, A. S., & Taschetto, A. S. (2009). What causes southeast Australia's worst droughts? *Geophysical Research Letters*, *36*(4). https://doi.org/10.1029/2008gl036801

Wallace, J. M., Smith, C., & Bretherton, C. S. (1992). Singular value decomposition of wintertime sea surface temperature and 500-mb height anomalies. *Journal of Climate*, *5*(6), 561-576. https://doi.org/10.1175/1520-0442(1992)005<0561:svdows>2.0.co;2

Zhang, L., Liu, Y., & Zhao, F. (2017). Singular value decomposition analysis of spatial relationships between monthly weather and air pollution index in China. *Stochastic Environmental Research and Risk Assessment*, *32*(3), 733-748. https://doi.org/10.1007/s00477-017-1491-z